Quasi-one-dimensional Fermi surface of $(TMTSF)_2NO_3$

W. Kang[1,*] and Ok-Hee Chung[2]
[1]*Department of Physics, Ewha W. University, Seoul 120-750, Korea*
[2]*Department of Physics, Sunchon University, Sunchon 540-742, South Korea*
(Received 28 October 2008; revised manuscript received 4 December 2008; published 21 January 2009)

Stereoscopic angular dependence of the interlayer magnetoresistance of the Bechgaard salt $(TMTSF)_2NO_3$ is investigated under pressure. This compound is believed to be a semimetal having the quasi-two-dimensional Fermi surface (FS) at low temperature. Previously, a field-induced spin-density-wave (FISDW) transition was reported at 8.5 kbar above ~20 T, which is atypical with a closed FS. We present strong evidence that the FS of this compound remains quasi-one-dimensional under moderate pressure even in the presence of anion ordering. The occurrence of the FISDW is therefore unsurprising. In addition, the possibility of an anion ordering along the *b* axis will be discussed.

DOI: 10.1103/PhysRevB.79.045115 PACS number(s): 71.18.+y, 72.15.Gd, 74.70.Kn

Bechgaard salts $(TMTSF)_2X$ [TMTSF =tetramethyltetraselenafulvalene and X is an inorganic anion] offer unique physics of the quasi-one-dimensional (Q1D) electron system. According to the temperature, pressure, and magnetic field to which a sample is subjected, various grounds states such as metallic, superconducting, spin-density wave (SDW), and field-induced spin-density-wave (FISDW) states can be realized in a sample. The anion ordering in noncentrosymmetric anion compounds puts additional effects on the common Q1D behaviors.[1] The magnetic orbital effect reduces the effective dimensionality of electrons and favors reappearance of the SDW state, FISDW.[2]

However, there are two compounds whose properties substantially depart from the typical Q1D behavior. One is $(TMTSF)_2NO_3$ when below the anion ordering temperature (T_{AO}) and the other is $(TMTSF)_2FSO_3$ when under moderate pressure and below the given anion ordering temperature. The angular magnetoresistance oscillations (AMROs) of $(TMTSF)_2FSO_3$ observed between 6 and 10 kbar can be explained in terms of Kartsovnik-Kajita-Yamaji (KKY) oscillations as evidence of the cylindrical quasi-two-dimensional (Q2D) Fermi surface (FS).[3–6] In this pressure range, this compound shows superconductivity below around 3 K but no FISDW up to 33 T.[7]

The FS of $(TMTSF)_2NO_3$ below T_{AO} has been regarded as small hole and electron pockets created by an anion ordering transition with a wave vector (1/2,0,0) (Refs. 8 and 9) that renders it semimetallic at low temperature.[10,11] At lower temperatures, an SDW state with incommensurate wave vector and imperfect nesting is formed ($T_{SDW} \simeq 9$ K at ambient pressure). The SDW state is suppressed by hydrostatic pressure, but the anion ordering remains. While the superconductivity has never been observed in $(TMTSF)_2NO_3$, an FISDW was recently observed above ~20 T at 8.5 kbar.[12] FISDW without superconductivity was also reported in Q1D $(DMET\text{-}TSF)_2AuCl_2$, which remains metallic down to 42 mK.[13] However, FISDW in a Q2D metal is unprecedented.

So, establishing the dimensionality of the title material, whether Q1D or Q2D, for the FISDW phenomena is pivotal to further understand the underlying physics of Bechgaard salts. A traditional way to determine the anisotropy of FS is by measuring angular dependence of the magnetic quantum oscillations, such as de Haas–van Alphen effect and Shubnikov–de Haas (SdH) effect.[14] However, these methods are of little use in studying Q1D materials because numerous magnetic oscillations are present whereas there is apparently no closed orbits in the Q1D FS.

In this context, a measurement of the AMRO is valuable in determining of the given FS and providing insights into dimension-related phenomena.[15] KKY oscillations are present if the FS is Q2D. Tangents of angular positions of the resistance *maxima* are proportional to integers and only weakly dependent on the azimuthal rotation.[5] In the Q1D case, the AMRO in a magnetic field perpendicular to the most conducting axis also shows fine structures, but tangents of angular positions of the resistance *minima* are linear to integers (Lebed resonances).[16,17] When the rotation plane approaches the one-dimensional (1D) conducting axis, the elevation angles from the conducting plane for the resistance minima approach zero and a complicated pattern including Danner-Kang-Chaikin (DKC) oscillations[18] and the third angle effect appears.[19,20] Moreover, exploration of three-dimensional AMRO will provide better pictures for the FS topology.[15]

We will show in this paper three-dimensional measurements of the AMRO of $(TMTSF)_2NO_3$ under moderate pressures. Even in the presence of anion ordering, all the oscillatory features in the angular magnetoresistance correspond to those arising from a system which comprises Q1D FS. However, our report does not exclude the possibility of Q2D FS pockets induced in the SDW state. Even so, our findings clearly demonstrate that the Q1D FS solely dominates the electronic properties of the title compound in the metallic state.

Single crystals of $(TMTSF)_2NO_3$ were synthesized electrochemically.[21] Electrical contact was made to the samples with 20 μm annealed gold wires with the carbon paste for the interlayer resistance R_{zz}. It is now well understood that anisotropy-related features in the MR are more pronounced in R_{zz}. Moreover, Q1D effects can be properly observed only in the R_{zz} as evidenced in Ref. 22. Special care was necessary when placing the contacts because the largest faces of $(TMTSF)_2NO_3$ crystals are *not* usually perpendicular to the c^* axis.[12,23] The right configuration was later confirmed by the shape of the angular magnetoresistance.

Pressure was applied in a clamped BeCu cell at room

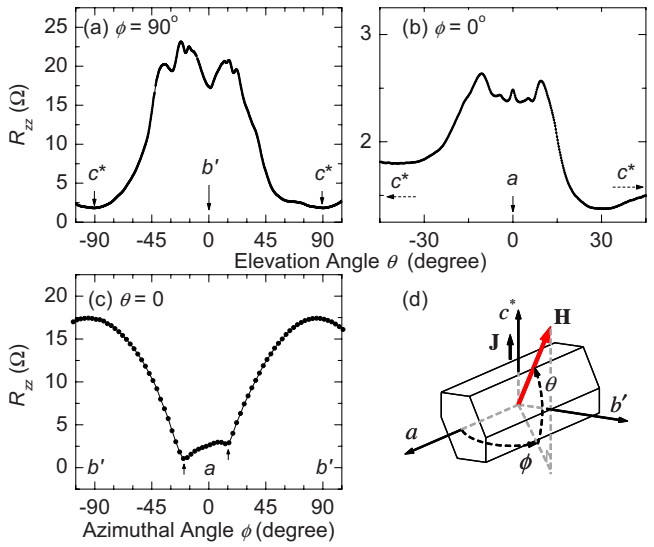

FIG. 1. (Color online) Angular magnetoresistance when the magnetic field rotates (a) in the $b'c^*$ plane (ϕ=90°), (b) in the ac^* plane (ϕ=0), and (c) in the ab' plane (θ=0). H=14 T, P =7.8 kbar, and T=1.6 K. $R_{zz}(\theta,90°)$ in (a) shows a series of dips in which tangent of the angles are linear to integers. $R_{zz}(\theta,0)$ in (b) shows typical DKC oscillation pattern with a coherence peak around θ=0°. The third angle effect in (c) has a width of $33.3° \pm 0.2°$. (d) depicts the definitions of angles with a typical $(TMTSF)_2NO_3$ crystal. Be sure that the symbol θ stands for the elevation angle from the conducting plane.

temperature with a hydraulic press. The pressure value was monitored with manganin manometer at room temperature and with pure tin (Sn) at low temperature.[24] Daphene 7373 oil was used as the pressure medium.[25] The angular dependence was measured with a two-axis rotator in a 14 T solenoid superconductor magnet. We checked the cooling rate effect (between 0.1 and 4.0 K/min) on low-temperature properties and verified its irrelevance to our results. Typical cooling rate was 1 K/min for the AMRO study.

At ambient pressure, an anion ordering transition took place at 42.9 K (from a maximum of $|dR_{zz}/dT|$) and the SDW transition at 9.2 K [from a maximum of $|d^2(\log R_{zz})/dT^2|$]. T_{AO} gradually increased with pressure and reached 48.8 K at 7.8 kbar. The AMRO measurements performed at three different pressures, 6.0, 7.0, and 7.8 kbar, gave essentially the same results. Even at 6.0 kbar, the samples remained fully metallic down to 0.4 K. This is slightly lower than that previously reported by Vignolles *et al.*[12] At 7.8 kbar, the sample showed a sharp resistance increase upon entering the FISDW at 12.3 T and 0.45 K. However, the threshold field was larger than 14 T at $T > 1.2$ K.

Figure 1 shows the typical AMRO when the magnetic field rotates (a) in the plane perpendicular to the a axis (ϕ =90°, $b'c^*$ plane), (b) in the plane defined by the a axis and the normal to the conducting layers (ϕ=0°, ac^* plane), and (c) in the plane parallel to the conducting layers (θ=0°, ab' plane). Whereas a series of resistance peaks and dips are present in Fig. 1(a), one cannot readily attribute them to either the KKY oscillations or the Lebed oscillations because only a few extreme values are available. In fact, tangents of both the maxima and the minima are consistently linear to integers. On the other hand, the features around the a axis for the field rotating in the ac^* plane as shown in Fig. 1(b) are ascertained as the DKC oscillations, the same as in metallic state of $(TMTSF)_2PF_6$ (Ref. 15) and $(TMTSF)_2ClO_4$.[18] The coherence peak of about 2.8° wide is well developed as the magnetic field approaches parallel to the most conducting a axis. The result observed in Fig. 1(b) is thus clear evidence for existence of a Q1D FS perpendicular to the a axis.

Figure 1(c) shows the interlayer magnetoresistance, $R_{zz}(0,\phi)$, with the magnetic field rotating in the conducting layers (ab' plane). The third angle effect[20] around the a axis is clearly observed (upward arrows) with its width of $33.3° \pm 0.5°$. This value is comparable to 28.6° in $(TMTSF)_2ClO_4$ at 1 bar[22] and 38.7° in $(TMTSF)_2PF_6$ at 8.4 kbar.[15] The third angle effect is an inherent feature associated with a topological effect of Q1D FS without involving the closed orbits. Therefore, the result of Fig. 1(c) is another manifest evidence in support the Q1D nature of $(TMTSF)_2NO_3$.

A more definitive way to determine the dimensionality of the FS responsible for the oscillatory behavior in Fig. 1 is to study the azimuthal angle dependence of the AMRO.[22,26] If the FS is a corrugated cylinder (Q2D), the magic angles θ_N of the KKY oscillations oscillate between maximum and minimum values determined by the semimajor and semiminor axes of the Q2D FS section without approaching zero. On the other hand, if the FS consists of Q1D sheets having weak corrugation along the second and the third directions, Lebed resonances occur when the B_y and B_z components satisfy the generalized magic angle condition.[17] As can be in the referenced formula, the magic angles $\theta_{p/q}$ of the Lebed resonances converge to zero as the field direction approaches the a axis (so the azimuthal angle ϕ approaches zero). In other words, all Lebed resonance features converge along the a axis.[15]

Figure 2(a) shows $R_{zz}(\theta,\phi)$ in an equirectangular projection. Resonant features can be clearly distinguished on the $b'c^*$ plane (ϕ=90), but the DKC features in Fig. 1(b) are hidden in this figure because their oscillatory amplitude is relatively small in comparison to the other features. However, the projection of the second derivatives of the angular magnetoresistance, $d^2R_{zz}/d\theta^2$ in Fig. 2(b) clearly shows the fine structure of resonant features continue to present even far from the b' axis, or equivalently close to the a axis. Amazingly, all the resonance lines merge into a narrow area around the a axis where a faint diamond shape structure develops, which are typical characteristics of the Q1D FS as evidenced in $(TMTSF)_2PF_6$.[15]

Figure 3 is a stereoscopic presentation of the $R_{zz}(\theta,\phi)$ in Fig. 2(a). The diamond shape around the a axis and the ridge from the coherence peaks are clearly visible along the horizontal plane. The resonant features converging around the a axis affirm existence of the Lebed resonance not the KKY resonance. Seen in upper right corner is the conductance surface of the same data.

Fitting the data of Fig. 1(a) to the Lebed resonance formula[17] gives 1.22 for the coefficient of p/q. Strikingly, this is about two times larger than 0.557 estimated from the low temperature (12 K) lattice parameters at 1 bar.[9] The co-

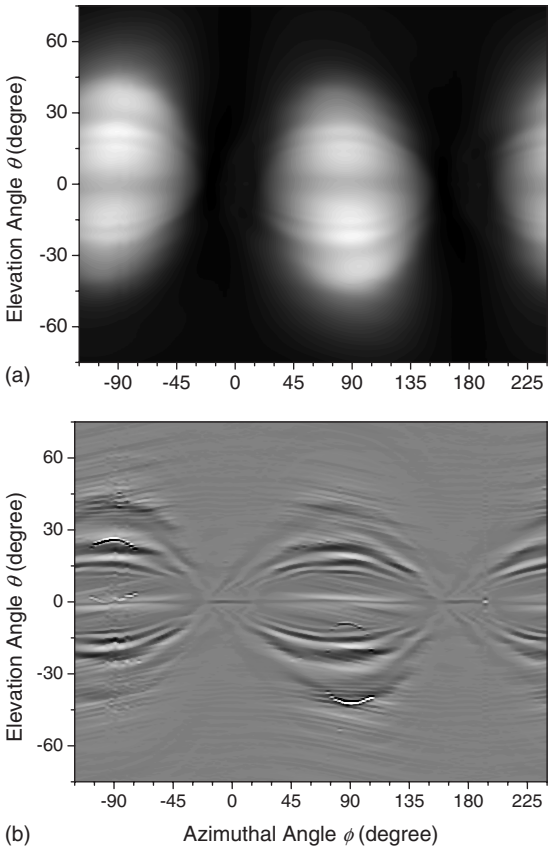

FIG. 2. (a) Equirectangular projection of $R_{zz}(\theta,\phi)$ of $(TMTSF)_2NO_3$. $H=14$ T, $P=7.8$ kbar, and $T=1.6$ K. (b) Equirectangular projection of $d^2R_{zz}(\theta,\phi)/d\theta^2$ at fixed ϕ. In (b), the valleys correspond to the angular region where $R_{zz}(\theta)$ is maximum and the ridges to where $R_{zz}(\theta)$ is minimum. The resonant features converge on the equator, 180° apart from each other. The noise is due to gear imperfections.

efficient for $(TMTSF)_2NO_3$ should be irrelevant to the anion ordering along the a axis. The most plausible explanation for the doubling of the coefficient is the presence of an "undetected" anion ordering along the b axis. In this case, the situation would be similar to $(TMTSF)_2ClO_4$ where the anion ordering wave vector is (0,1/2,0). Both the similarity of the conductance surface in Fig. 3 and the periodicity of the Lebed resonance features strongly support the possibility of an additional ordering of NO_3 anions. According to Barrans *et al.*,[9] the reflection intensity due to the anion ordering along the a axis is 10 or 100 times weaker than main reflection. Although the anion ordering along the b axis occurs, it would give much weaker intensity if it is less favorable than that along the a axis. Considering the cooling rate of 1 K/min used in this study, the additional ordering along the b axis may not result from the relaxation of anions across T_{AO}, which is important for $(TMTSF)_2ClO_4$. There was no apparent sign for the change of the anion ordering by pressure as in $(TMTSF)_2ReO_4$.[27] At the moment, it is not possible to determine whether this additional ordering of anions is induced by pressure or present from the ambient pressure. AMRO study at ambient pressure is not useful either because of the SDW.

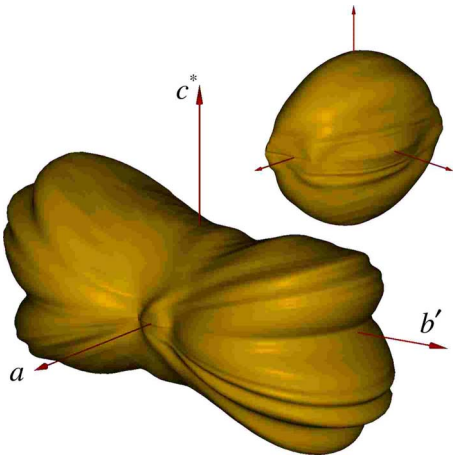

FIG. 3. (Color online) Stereographic representation of $R_{zz}(\theta,\phi)$ of $(TMTSF)_2NO_3$. The distance from the origin to a point on the surface is the magnetoresistance added to a 10 Ω isotropic resistance sphere. The diamond shape around the a axis and the ridge from the coherence peak within it are clearly discerned. The upper right picture shows the conductance of the same data.

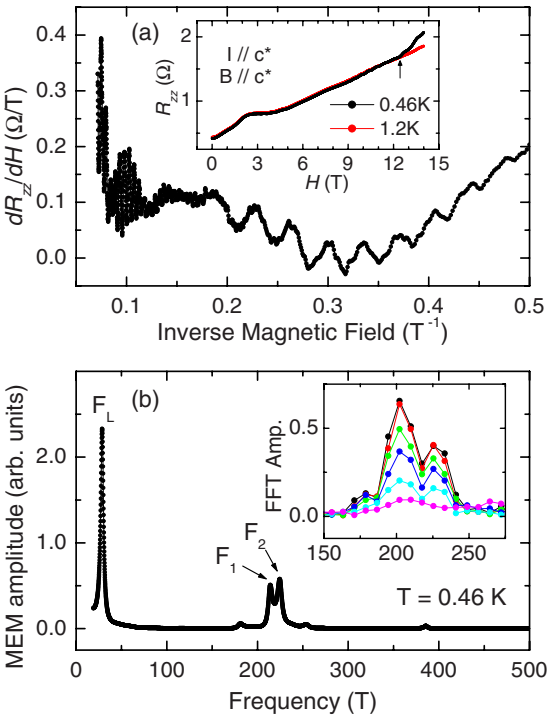

FIG. 4. (Color online) (a) The first derivative of magnetoresistance, dR_{zz}/dH is plotted at $T=0.46$ K as a function of inverse field. R_{zz} for two temperatures is plotted as a function of magnetic field in the inset, in which the occurrence of FISDW is observed as a sudden change at 12.3 T at 0.46 K. (b) FT spectrum obtained by the maximum entropy method which enhances the resolution of peaks in exchange of the peak shape. Slow oscillations with 28.7 T are dominant below 5 T while fast ones with two frequencies, 214 and 225 T, develop above 5 T. Temperature dependence of the ordinary FFT spectrum for two frequencies is showed in inset. Temperatures are 0.46, 0.6, 0.9, 1.2, 1.9, and 2.5 K from top to bottom.

Contrary to a previous report by Vignolles *et al.*[12] in which additional oscillations were observed not in the metallic state but in the FISDW state above ~20 T at 8.5 kbar, we readily observed fast oscillations in both the metallic and FISDW states even in low tesla fields. Figure 4 shows the field dependent magnetoresistance and its first derivative as a function of inverse field at 0.46 K. As is seen Fig. 4(a), slow oscillations occur from around 2 T up and fast oscillations become apparent around 5 T. The overall shape of the fast oscillations is modulated by a slowly varying envelope. Figure 4(b) shows the Fourier transformed (FT) spectra of the same data using the maximum entropy method. There are three major peaks in the spectrum. Among them, two high-frequency peaks at 214 and 225 T correspond to the fast oscillations above 7 kbar in Ref. 12. While the fast oscillations in Ref. 12 were found only in the FISDW state ($\gtrsim$20 T at 8.5 kbar), they were observed in both metallic and FISDW state in this study, reminiscent to $(TMTSF)_2ClO_4$ (Ref. 28) or $(TMTSF)_2ReO_4$.[29] In the inset of Fig. 4(b) temperature dependence of the double peak is plotted with fast Fourier transform (FFT) method. The double peak of the fast oscillations is observable up to 1.9 K. The 60 T oscillations widely observed in the low-pressure SDW phase disappear above the threshold pressure.[12] Although the 60 T is very close to the frequency of the FISDW cascade in other salts, the absence of the 60 T oscillations at 7.8 kbar confirms that they are related to the ambient pressure SDW not to the FISDW. Unexpectedly, another type of slow oscillations with a frequency of 28.7 T was observed in the best samples. This has never been reported in either metallic[12] or SDW states of $(TMTSF)_2NO_3$ before.[30,31]

Here, we need to discuss further the origin of the Q2D-like oscillations. In our AMRO results, there is no single indication to prove existence of Q2D FS in the metallic state. Then, it is more probable that the SdH-type oscillations are so-called "rapid oscillations (RO)" widely observed in the Q1D Bechgaard salts.[28] Although the Stark interference effect is the most plausible explanation for RO which can be formed without closed orbits, the origin is not clarified yet.

In conclusion, our inquiry provides manifest evidence for the existence of Q1D FS in $(TMTSF)_2NO_3$ under pressures larger than the critical pressure of 6.0 kbar. This is evident even in the presence of the anion ordering, thus suggesting the appearance of the FISDW likely. Contrarily, we found no evidence to support the existence of the FISDW in Q2D semimetals.[12] Without excluding the presence of the Q2D FS pockets in the low-pressure SDW state, our study makes obvious that the Q1D FS dominates the metallic properties of the title compound in the absence of the SDW. Stereoscopic measurements of the AMRO were vital in determining the dimensionality of the FS. In addition, the periodicity of Lebed type resonances and the overall stereoscopic features of $R_{zz}(\theta,\phi)$ suggest an additional anion ordering along the b axis should be present as in $(TMTSF)_2ClO_4$. Whether the b axis ordering persists down to low pressure can only be clarified by further structural analysis between T_{SDW} and T_{AO} since ARMO is not sharp enough in this temperature range. Lastly, the absence of superconductivity is still an unexplained phenomenon in this compound.

This work was supported by the Korea Science and Engineering Foundation (Grants No. R01-2007-000-20576-0 and No. R11-2008-053-02002-0 for W.K. and Grant No. R01-2007-000-11915-0 for O.-H.C.) and by the Korea Research Foundation (Grant No. R14-2003-027-01000-0). We thank K. Murata for making the Daphene 7373 oil available and Y. J. Jo and H. Kang for sample preparation.

*wkang@ewha.ac.kr

[1] A. G. Lebed, *Organic Conductors and Superconductors*, Series in Materials Science Vol. 100 (Springer-Verlag, Berlin, 2008).
[2] P. M. Chaikin, Phys. Rev. B **31**, 4770 (1985).
[3] M. V. Kartsovnik, P. A. Kononovich, V. N. Laukhin, and I. F. Schegolev, JETP Lett. **48**, 541 (1988).
[4] K. Kajita, Y. Nishio, T. Takahashi, W. Sasaki, R. Kato, and H. Kobayashi, Solid State Commun. **70**, 1189 (1989).
[5] K. Yamaji, J. Phys. Soc. Jpn. **58**, 1520 (1989).
[6] The angular positions θ_N of the KKY resonance peaks are given as (Ref. 5) $ck_F \cot\theta_N=\pi(N-\frac{1}{4})-C$, where c is the distance between adjacent conducting planes, k_F is the wave vector whose projection is on the Fermi surface, and N is the index of resonance. C is a constant depending on the azimuthal angle.
[7] W. Kang, O. H. Chung, Y. J. Jo, H. Kang, and I. S. Seo, Phys. Rev. B **68**, 073101 (2003).
[8] J. P. Pouget, R. Moret, R. Comes, and K. Bechgaard, J. Phys. (Paris), Lett. **42**, L543 (1981).
[9] Y. Barrans, J. Gaultier, S. Brachetti, P. Guionneau, D. Chasseau, and J. M. Fabre, Synth. Met. **103**, 2042 (1999).
[10] P. M. Grant, Phys. Rev. Lett. **50**, 1005 (1983).
[11] D. Jérome, C. R. Acad. Sci., Ser. II: Mec., Phys., Chim., Sci. Terre Univers **317**, 569 (1993).
[12] D. Vignolles, A. Audouard, M. Nardone, L. Brossard, S. Bouguessa, and J. M. Fabre, Phys. Rev. B **71**, 020404(R) (2005).
[13] N. Biškup, J. S. Brooks, R. Kato, and K. Oshima, Phys. Rev. B **60**, R15005 (1999).
[14] D. Shoenberg, *Magnetic Oscillations in Metals* (Cambridge University Press, Cambridge, 1984).
[15] W. Kang, T. Osada, Y. J. Jo, and H. Kang, Phys. Rev. Lett. **99**, 017002 (2007).
[16] A. G. Lebed, Pis'ma Zh. Eksp. Teor. Fiz. **43**, 137 (1986) [JETP Lett. **43**, 174 (1986)].
[17] The Lebed's original suggestion (Ref. 16) was extended to give the resonance angles $\theta_{p/q}$ for arbitrary azimuthal plane such as (Refs. 32 and 33) $\frac{B_y}{B_z}=\cot\theta_{p/q}\sin\phi=\frac{p}{q}\frac{b\sin\gamma}{c\sin\beta\sin\alpha^*}-\cot\alpha^*$, regardless of B_x. Here, b, c, β, γ, and α^* are lattice parameters and p and q are small integers.
[18] G. M. Danner, W. Kang, and P. M. Chaikin, Phys. Rev. Lett. **72**, 3714 (1994).
[19] H. Yoshino, K. Saito, K. Kikuchi, H. Nishikawa, K. Kobayashi, and I. Ikemoto, J. Phys. Soc. Jpn. **64**, 2307 (1995).
[20] T. Osada, S. Kagoshima, and N. Miura, Phys. Rev. Lett. **77**, 5261 (1996).

[21] J. R. Ferraro and J. M. Williams, *Introduction to Synthetic Electrical Conductors* (Academic, New York, 1987).
[22] W. Kang, Phys. Rev. B **76**, 193103 (2007).
[23] N. Biškup, M. Basletić, S. Tomić, B. Korin-Hamzić, K. Maki, K. Bechgaard, and J. M. Fabre, Phys. Rev. B **47**, 8289 (1993).
[24] L. D. Jennings and C. A. Swenson, Phys. Rev. **112**, 31 (1958).
[25] K. Murata, H. Yoshino, H. O. Yadav, Y. Honda, and N. Shirakawa, Rev. Sci. Instrum. **68**, 2490 (1997).
[26] M. V. Kartsovnik, Chem. Rev. (Washington, D.C.) **104**, 5737 (2004).
[27] R. Moret, S. Ravy, J. P. Pouget, R. Comes, and K. Bechgaard, Phys. Rev. Lett. **57**, 1915 (1986).
[28] X. Yan, M. J. Naughton, R. V. Chamberlin, S. Y. Hsu, L. Y. Chiang, J. S. Brooks, and P. M. Chaikin, Phys. Rev. B **36**, 1799 (1987).
[29] W. Kang, J. R. Cooper, and D. Jérome, Phys. Rev. B **43**, 11467 (1991).
[30] N. Biškup, L. Balicas, S. Tomić, D. Jérome, and J.-M. Fabre, Phys. Rev. B **50**, 12721 (1994).
[31] A. Audouard, F. Goze, J.-P. Ulmet, L. Brossard, S. Askénazy, and J. M. Fabre, Phys. Rev. B **50**, 12726 (1994).
[32] I. J. Lee and M. J. Naughton, Phys. Rev. B **57**, 7423 (1998).
[33] A. G. Lebed and M. J. Naughton, Phys. Rev. Lett. **91**, 187003 (2003).